Proceedings of ICFDP7:
Seventh International Congress on Fluid Dynamics and Propulsion
December 18 – 20, 2001, Cairo, Egypt

ICFDP7-2001046

A DOPPLER SENSOR FOR HIGH-RESOLUTION MEASUREMENTS OF THE TURBULENT WALL PRESSURE AT HIGH-REYNOLDS NUMBERS

M. Daoud/Michigan State University **A. Naguib**/Michigan State University

Y. Li/Michigan State University

ABSTRACT

A new unsteady-surface-pressure measurement technique is demonstrated. The technique utilizes the Doppler frequency shift as the basic sensing mechanism. The frequency shift is experienced by a focused laser beam reflected off the aluminized top of a flexible polymer diaphragm subjected to the unsteady pressure. A prototypical sensor based on this concept, with 2-mm sensing size, is developed and characterized. The results reveal a sensor diaphragm sensitivity of about 0.04 μm/Pa and useful frequency range of $100 < f < 4000$ Hz. Furthermore, wall-pressure spectra obtained using the new sensor in a low-Reynolds-number turbulent boundary layer agree well with those obtained from a commercial electret microphone. The new approach has the potential to realize sensor arrays with less than 500 μm diameter for use in high Reynolds number diagnostics.

INTRODUCTION

Measurement of the unsteady surface pressure signature produced by a wide range of turbulent flows is significant for a number of reasons. First, understanding and predicting flow and structure behavior in applications involving flow/structure interaction in general, and flow-induced vibrations in particular, depend on knowledge of the normal flow stresses acting on the surface. Second, in modern active flow control applications, it is desirable to measure the 'flow state' and adapt the control accordingly. Sensing of the surface pressure provides an option whereby flow influences can be detected on the surface without the interfering effect of inserting probes into the flow. Finally, array measurements of the surface pressure could be used to obtain the wall vorticity flux: a quantity that is important not only for interpretation of flow physics but also for flow computation using vortex methods.

When it comes to sensing the surface pressure at high Reynolds numbers, current techniques for measuring the surface pressure are generally limited by their spatial resolution. In particular, in test facilities capable of establishing a turbulent boundary layer at Reynolds numbers comparable to those encountered over a ship, submarine, or airplane, the viscous length scale (ν/u_τ) is typically as small as a few to tens of microns. Gravante *et al*. (1998) showed that a non-dimensional sensor size ($d^+ = du_\tau/\nu$) of 18 or smaller is sufficient to resolve the influences of the wall-pressure-producing eddies. Thus, sensors with diameters less than 0.5 mm or so are generally required to fully resolve the wall-pressure signature at high Reynolds numbers. Additionally, if it is desired to measure maps of the wall-vorticity flux, a sensor array with small inter-sensor spacing is required in order to accurately estimate the spatial gradients of the surface pressure. The cost and implementation complexity of such an array should also be kept to a minimum if the measurement technique is to be viable and of practical use.

Historically, measurement of the turbulent surface pressure has been accomplished using capacitive microphones. High-quality capacitive microphones, such as Brüel and Kajer and Larson and Davis, have the advantage of high-sensitivity, flat frequency characteristics (typically from 20 Hz – 20 kHz) and known response. However, the smallest size microphone of this type is 3.175 mm (1/8") in diameter. Farabee and Casarella (1991) overcame this problem by using a pinhole on top of a 1/8" microphone to limit d to 0.79 mm. However, with this approach, the inter-sensor spacing remains limited by the sensor diameter. Moreover, the cost of these high-quality microphones (order of $2k per channel) and the complexity of routing tens of wires through a test model render these sensors unsuitable for array applications and vorticity flux measurements.

To overcome some of the limitations of high-quality microphones in multi-sensor applications, significantly cheaper, yet stable, highly-sensitive and smaller, electret type microphones have been used by a number of researchers. For example, Snarski and Lueptow (1995) and Gravante *et al*. (1998) used miniature hearing-aid microphones from Knowles. These sensors can be implemented in arrays in a cost-effective manner at an inter-sensor spacing of 1- 4 mm. However, the microphone units are not calibrated individually by the manufacturer and the sensitivity and phase response of these microphones can change significantly with frequency. Furthermore, the need to electrically wire these sensors makes it inconvenient to implement them in a sensor array.

One disadvantage of capacitive and electret microphones is that they can't measure pressure fluctuations below 10 – 20 Hz. An alternative sensor type that has a bandwidth extending from DC to 20 kHz is the silicon-based piezoresistive pressure transducer. Sensors of this type are available commercially (e.g., from Kulite or Entran) in sizes as small as about 1 mm. The sensitivity of these sensors, however, is about two orders of magnitude lower than that of 1/8" capacitive microphones. However, because of their fairly small size, Kulite sensors have been used successfully to measure the one-point wall vorticity flux in a moderate Reynolds number boundary layer (Honkan and Andreopoulos, 1993). Extension of the usability of current commercial piezoresistive pressure transducers to high Reynolds number flows and array applications is limited by the sensor's size and the cost/complexity of multi-sensor systems (a single transducer costs about $500).

Perhaps MEMS (Micro Electro Mechanical Systems) technology holds the most promise for realizing spatially and temporally resolved measurements of the surface pressure at high Reynolds numbers. MEMS piezoresistive sensors have been fabricated and tested by Löfdahl *et al*. (1994), Sheplak *et al*. (1998), and Naguib *et al*. (1999). The latter authors fabricated sensors with square diaphragm as small as 510 μm on the side. These sensors possessed a sensitivity that was an order of magnitude higher than that of commercial Kultie sensors. However, the frequency response of the sensors was limited to less than a few kHz. It is expected that it will take several years of development for MEMS sensors to mature. However, the technology may ultimately lead to the development of self-contained sub-500-μm surface-pressure sensor arrays, including on-chip electronics for providing power and signal conditioning to the sensors as well as wireless transmission of the measurement signals.

NOMENCLATURE

d : Sensing Diameter
f : Frequency
f_D : Doppler Frequency
K_δ : Sensor Deflection Static Sensitivity
p : Wall Pressure
r : Resolution Parameter
t : Time
u_τ : Friction Velocity
v : Velocity of Sensor Diaphragm
Δf_D : Measurement Resolution of Doppler Frequency
δ : Deflection of Sensor Diaphragm
$\phi_{\delta\delta}$: Deflection Power Spectrum
ϕ_{pp} : Wall-Pressure Spectrum
λ : Wavelength of Laser Light
ν : Kinematic Viscosity

OBJECTIVES

The goal of this work is to demonstrate a new surface-pressure sensor concept that is based on the Doppler frequency shift. Because the technique utilizes a laser beam that can be focused to a spot size of a few to tens of microns, sensors of this new type can potentially be constructed with diameters less than 500 μm and implemented in an array with sub-mm inter-sensor spacing. In this paper, only results pertaining to the development and characterization of a 2-mm-diameter single sensor element are discussed. Additionally, wall-pressure spectra obtained from measurements using the new sensor in a low-Reynolds-number turbulent boundary layer are presented and compared to the spectra measured by a commercial electret type microphone.

CONCEPT AND DETAILS OF SENSOR SYSTEM

The Primary sensing element of the Laser Doppler Microphone (LDM) consists of a thin polymer diaphragm with a reflective upper surface attached to a plug substrate on top of a hole, as seen in Figure 1. Under the action of the unsteady flow pressure, the diaphragm experiences time-dependent deflection on top of the hole (note that the spatial resolution of the sensor is, thus, determined by the hole diameter, d). The instantaneous wall-normal velocity ($v(t)$) of the diaphragm is measured using the Doppler frequency shift of a laser beam incident on the reflective side of the pressure-sensing foil. The corresponding deflection ($\delta(t)$) is obtained from time integration of $v(t)$. Since the wall pressure ($p(t)$) acting on the diaphragm is directly proportional to δ, within the elastic limit of the diaphragm and its bandwidth, one may obtain p from:

$$p(t) = \frac{1}{K_\delta}\int v(t)dt + C\,, \qquad [1]$$

where K_δ is the deflection static sensitivity of the diaphragm (in units of μm/Pa) and C is an integration constant equal to the local mean surface pressure.

Figure 2. shows a schematic of the sensor plug design adopted for use in the experiments described here. The plug consists of four main components: face plate, plug body, foil ring and back chamber. Unlike the schematic shown in Figure 1, it was decided to use a face plate, or cover, on top of the pressure sensor in order to reduce the sensing hole diameter without affecting the hole size beneath the diaphragm. This

pinhole arrangement provides a means for obtaining high spatial resolution without sacrificing sensor sensitivity. The adoption of this geometry was necessary because of the very low surface-pressure fluctuation levels ($p_{rms} \approx 0.5$ Pa) encountered in the low-Reynolds-number wind tunnel tests conducted here. Such a pinhole would not be needed in a typical high Reynolds number test facility, where the pressure fluctuations would be one to two orders of magnitude higher than encountered in the current tests.

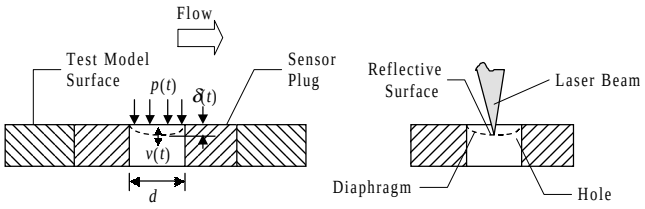

Figure 1. Terminology and Principle of Operation of the LDM Sensor.

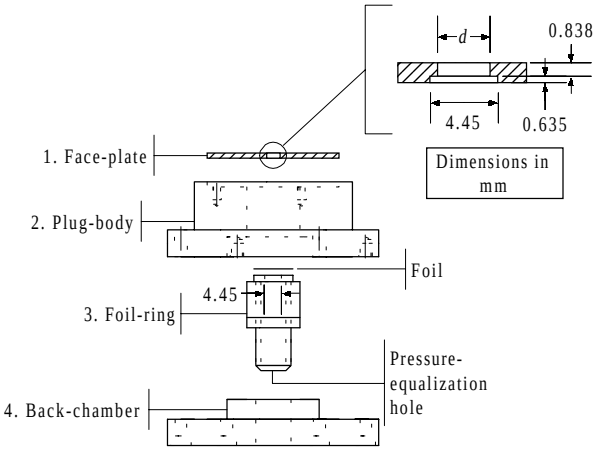

Figure 2. Schematic of the LDM Sensor Plug Design.

A picture of the optical system used to measure the LDM diaphragm velocity is provided in Figure 3. The light source for the Doppler system is a Uniphase 20 mW polarized He-Ne laser with a wavelength (λ) of 633 nm. The laser beam passes through a ¼λ (QP) plate, which in combination with the laser-head polarizer stops any reflected laser light from entering the laser tube. After the ¼λ plate, the laser beam is split into 'measurement' and 'reference' beams using a 50/50 cube beam splitter (BS1). Each of these two beams is passed through an Interaction Corp. acousto-optic modulator, model AOM-40, for independent frequency biasing to eliminate the sign ambiguity of the Doppler frequency shift. The acousto-optic modulators are driven using an Interaction Corp. dual-channel frequency synthesizer, model DFE. The use of two independent AOM units enables the attainment of a frequency bias between the measurement and reference beams in steps of ±10 kHz. Furthermore, the single-crystal driver of both units ensures temperature-independent frequency shift. The frequency-shifted measurement beam is directed through a second beam splitter (BS2), off mirrors M1 and M2, and through a 500-mm focal-length achromatic lens (AL) towards the pressure-sensor diaphragm. The achromatic lens is used to decrease the spot size of the beam to approximately 0.4 mm.

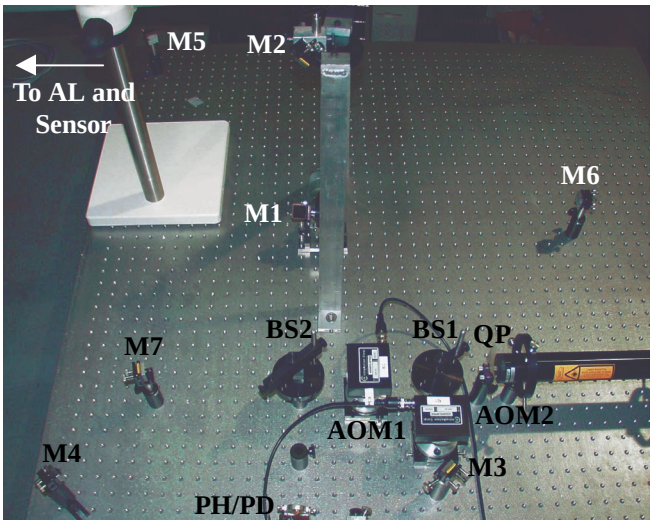

Figure 3. Optical System Setup

To obtain an electric signal with a frequency equal to the Doppler frequency shift, the reference beam is reflected off a number of mirrors (M3 through M7) to redirect it towards BS2 (see Figure 3), where it recombines with the measurement beam *after* reflection from the pressure sensor foil. The use of multiple mirrors to redirect the reference beam enables adjustment of the optical path length of the beam to ensure that the mismatch in path length of both beams is within the coherence length of the laser. Finally, both beams are mixed ('hetrodyned') on the surface of a low-noise (unbiased) photodetector (PD), after passing through a pinhole (PH) for minimizing extraneous light effects.

To measure the frequency of the photodetector signal, an FFT-based approach is used. The signal is acquired using a 12-bit, 50 Mega sample/s, two-channel, one Mega-sample data memory, Gagescope CS1250 data acquisition card from Gage. In the traditional FFT approach, the power spectrum of each data record of the photodetector signal is computed using the FFT. Subsequently, the Doppler frequency is determined to be that corresponding to the maximum spectrum magnitude. The resolution by which the Doppler frequency is determined using the spectrum peak technique is given by $\Delta f_D = 1/T_{rec}$, where T_{rec} is the duration of the acquired photodetector signal.

To reduce the LDM data record duration without sacrificing the Doppler frequency resolution, a centroid-based

approach for detecting the spectrum peak location with 'sub-bin' resolution was employed. The capability of the approach is demonstrated in Figure 4 by comparison to frequency measurements based on the peak-detection method. The results in the figure were obtained using a sinusoidally oscillating mirror that was placed as a target for the Doppler system (i.e., in place of the sensor diaphragm). The significant enhancement in resolution over the traditional FFT approach is evident. Based on this test, it is found that a resolution enhancement of about 1:20-25 is obtained when using the centroid approach.

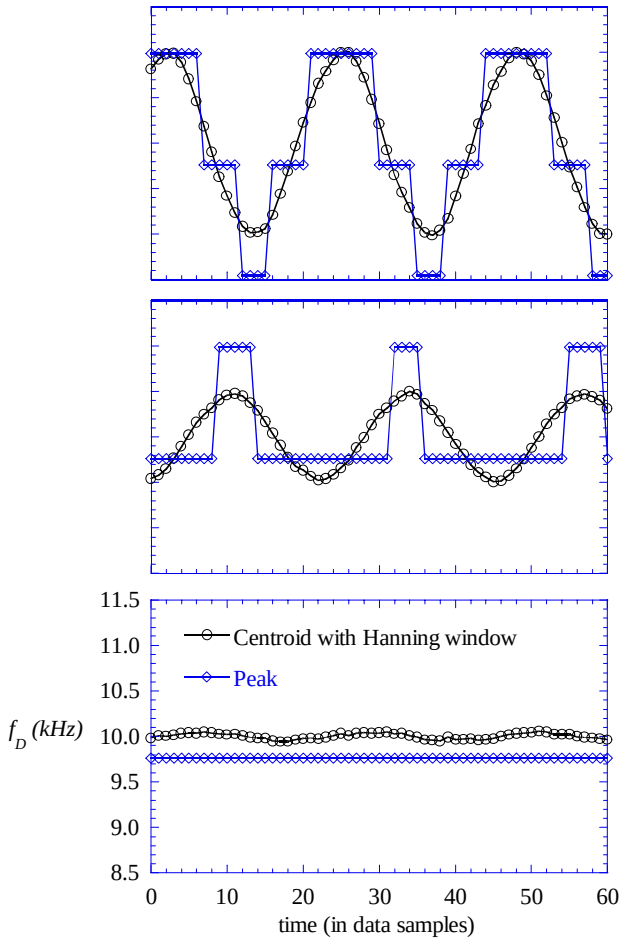

Figure 4. Demonstration of Doppler Frequency Resolution Enahncement using the Centroid Method

Each LDM data record yields a Doppler frequency shift. Typically, 256 to 1024 such records are acquired at a desired sampling rate to obtain a Doppler frequency time series, from which a diaphragm velocity (v) time series is obtained using the equation:

$$v = \frac{\lambda}{2} f_D, \qquad [2]$$

where, f_D is the Doppler frequency shift in Hz. This velocity time series is subsequently integrated, after removal of its average value to avoid the linear-drift associated with the integration of the DC component. Initially, integration was performed in the time domain using the trapezoid rule. However, it was later realized that the accuracy of time integration was not acceptable for frequencies approaching the Nyquist frequency where too few data points represented each cycle. This is demonstrated in Figure 5, where the displacement spectrum obtained from a sample measurement using time integration is divided by the velocity spectrum. The result is compared to the spectrum of an ideal integrator (given by: $1/\omega^2 = 1/(2\pi f)^2$). One can clearly see the systematic attenuation at the high frequency end of the spectrum resulting from integration in the time domain. Hence, integration was implemented as a frequency-domain filter with each velocity time series Fourier-transformed and multiplied by the complex factor $e^{-j\pi/2}/\omega$; i.e., the magnitude of the transform is scaled by the frequency and the phase angle is delayed by 90 degrees. The result is inverse Fourier transformed to obtain the diaphragm displacement time series, $\delta(t)$.

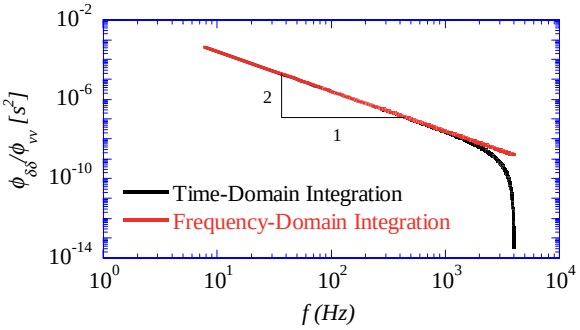

Figure 5. Comparison between Discrete-Time and Ideal (Frequency-Domain) Integration

SENSOR CALIBRATION

To obtain the frequency dependence of K_δ, the LDM sensor is mounted next to a commercial Panasonic electret microphone, type WM-61A in a nominally two-dimensional flow. The sensitivity of the Panasonic microphone is 17 mV/Pa and it has a sensing diameter of 2.032 mm. The calibration flow field is that of a separating/reattaching flow behind a 19-mm fence that is mounted on the side wall of a wind tunnel test section. The two sensors are located close to the test section centerline and at the same streamwise location of approximately twelve fence heights behind the fence. The spacing of the two sensors in the spanwise direction is 1.16 fence heights, while the full span of the fence extends across the test-section width of 22.6 fence heights. Using a second Panasonic Microphone in place of the Doppler sensor, it was verified that in fact the wall-pressure spectrum seen by both sensors is the same. It should be noted that this calibration procedure provides the frequency dependence of the sensor's sensitivity (K_δ) but not its phase.

A sensor with pinhole diameter of 2.032 mm was calibrated at a flow velocity of 6 m/s. This diameter was selected to be the same as that of the Panasonic microphone to ensure that spatial averaging effects of the high-frequency turbulent pressure fluctuations are the same for both sensors. The *static* pressure inside the test section was equalized across the LDM sensor foil with the aid of a pitot probe that was mounted in the wind tunnel with its static port located at the streamwise position of the sensor. Equalization was achieved by connecting the static port of the pitot tube to the back chamber of the LDM sensor through a small tank with a volume of 2000 cc. The tank was used to damp any pressure fluctuations above 0.1 Hz and, thus, prevent them from equalizing across the sensor's foil. For both the LDM and Panasonic sensors, 32 time series were used to obtain the average spectrum. Each time series contained 1024 points, sampled at 8,000 Hz. For the LDM sensor, each of the 1024 points represented the velocity of the sensor diaphragm, which was obtained from 512-point records of the photodetector signal sampled at 5 Mega samples/s. The Doppler signal was frequency shifted by 100 kHz using the acousto-optic modulators.

The dynamic calibration of the sensor is obtained using the following equation:

$$K_\delta = \sqrt{\frac{\phi_{\delta\delta}}{\phi_{pp}}} \ (\mu m/Pa) \qquad [3]$$

where, $\phi_{\delta\delta}$ is the LDM spectrum in μm^2 and ϕ_{pp} is the Panasonic spectrum in Pa^2. Using equation [3], the measured sensitivity of the Doppler sensor is obtained and plotted in Figure 6. It should be noted that, ideally, K_δ, or foil deflection per unit pressure, is expected to be constant from DC up to the bandwidth of the sensor. The latter depends on the resonant frequency of the foil (ω_r). The larger ω_r, the wider the bandwidth. The response displayed in Figure 6 seems to exhibit a behavior consistent with that expected for frequencies larger than 100 Hz. Within this range, a flat sensitivity value of approximately 0.04 μm/Pa is maintained up to the vicinity of the resonant peak (depicted at 3200 Hz). This behavior (for f >100 Hz) seems to be represented well using a second-order system response, as seen in Figure 6. A 5th order polynomial fit, however, gives a better description of the resonant peak. In the boundary layer measurements described below, a composite-fit (2nd order system for most of the frequency range and a 5th order polynomial in the vicinity of the peak) was used to convert the foil displacement to pressure. The use of the frequency-dependent sensitivity in the data conversion process eliminates the need to damp the resonant peak in order to obtain a flat response over the frequency range of interest.

For frequencies less than 100 Hz, the pressure sensor sensitivity appears to increase with decreasing frequency (Figure 6). This trend can't be descriptive of the actual K_δ behavior, which should be flat down to zero frequency. It is more likely that the low-frequency characteristics observed in Figure 6 are caused by inadequate Doppler frequency resolution for pressure oscillations below 100 Hz. To elaborate, consider a sinusoidal deflection of the sensor foil with frequency ω_o and amplitude a_o, caused by pressure oscillations with amplitude p_o. The corresponding diaphragm velocity will also be sinusoidal with the same frequency but amplitude of $a_o\omega_o$. This produces a sinusoidal Doppler frequency shift with amplitude $(2/\lambda)a_o\omega_o$. One may then define a resolution parameter (r), as the ratio of the frequency shift to the frequency resolution of the Doppler detection system (Δf_D):

$$r = \frac{(2/\lambda)a_o\omega_o}{\Delta f_D} = \frac{(2/\lambda)p_o K_\delta \omega_o}{\Delta f_D} = \frac{2p_o K_\delta \omega_o}{\lambda \Delta f_D} \qquad [4]$$

Equation [4] shows that the measured frequency shift decreases with decreasing pressure-oscillation frequency (assuming p_o to be constant). Presumably, the decrease in Doppler shift with diminishing frequency reaches a point where r is of order one; i.e., the frequency shift is of the order of the measurement resolution, and the foil velocity, and hence its displacement, cannot be resolved properly. According to equation [4], this 'breakdown' frequency is lower for flows with larger pressure fluctuations (p_o). Moreover, it is possible to further decrease the value of this frequency by using more sensitive foils, employing a shorter wavelength laser, or enhancing the measurement resolution of the Doppler frequency, as seen from equation [4].

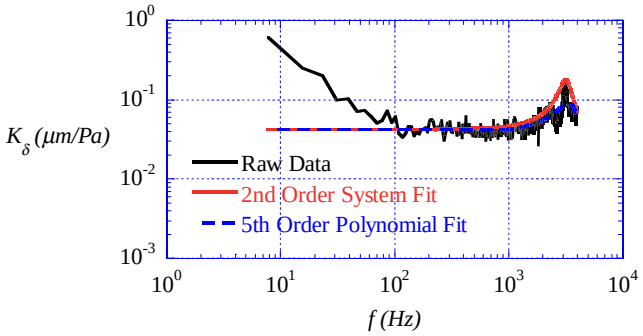

Figure 6. Dynamic Response of the LDM Sensor

BOUNDARY LAYER MEASUREMENTS

The calibrated LDM sensor was used to measure the surface pressure fluctuations in a turbulent boundary layer. This was done in order to verify the sensor operation in a flow field different from that used in the calibration. The boundary layer was established on the side wall of the wind tunnel test section by placing a 0.229 m-wide × 0.279 m-long sand-paper strip at the entrance to the test section. The measurement station was approximately 1.5 m downstream of the strip and the free-stream velocity was 8 m/s. Since the primary purpose of this work is to compare the new sensor to the Panasonic

microphone, the boundary layer characteristics were not documented.

Figure 7 shows the wall-pressure spectrum measured by the new sensor compared to that captured by the Panasonic microphone. A good agreement is obtained between the spectra over a frequency range of 300 Hz < f < 4000 Hz.

On the other hand, the deviation between the spectra at low frequencies is seen to occur at a frequency that is higher than the valid calibration range (f > 100 Hz). This is consistent with the earlier discussion concerning the measurement resolution of the Doppler frequency. The level of pressure fluctuation in the turbulent boundary layer is significantly lower than that encountered in the separating/reattaching flow used in calibration. Therefore, according to equation [4], one would expect the resolution factor r to reach a value of order one in the boundary layer case at a higher frequency than in the fence flow.

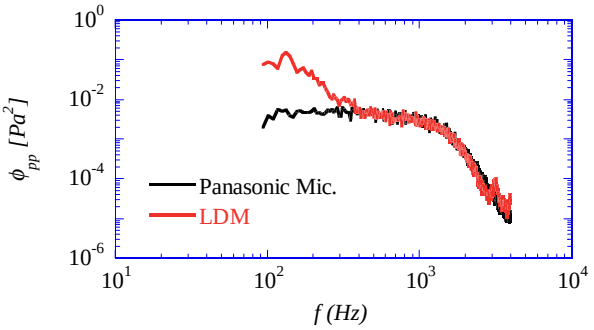

Figure 7. Comparison between the Spectra Measured by the LDM Sensor and Panasonic Microphone in the Turbulent Boundary Layer Flow

CONCLUSIONS

A new optical unsteady-wall-pressure sensor has been developed and characterized. The sensor principle of operation is based on the Doppler frequency shift and is believed to have a good potential for realizing high-spatial-resolution sensor arrays. The sensor operation requires a Doppler frequency measurement resolution that is significantly better than that typically used in LDV (Laser Doppler Velocimetery). Therefore, a centroid-based approach is used to achieve more than an order of magnitude enhancement of the resolution of the FFT-based method used for frequency detection.

A prototype of the sensor has been characterized by comparing its output to that of a commercial Panasonic microphone while embedded in a two-dimensional separating/reattaching flow. The results revealed a sensor sensitivity of 0.04 μm/Pa and a useful frequency range of 100-4000 Hz. While the higher frequency is not limited by the sensor characteristics (this was simply the Nyquist frequency in the experiments conducted), the lower one is believed to represent the measurement resolution-limit of the Doppler frequency. This limit can be improved using more flexible diaphragm material or shorter wavelength laser.

The calibrated sensor was used to conduct measurements of the surface pressure spectrum beneath a turbulent boundary layer. The results showed good agreement with the commercial microphone over the frequency range 300 < f < 4000 Hz.

ACKNOWLEDGMENTS

The authors would like to express their appreciation of the support of the Office of Naval Research of this work, monitored by Dr. L. Patrick Purtell.

REFERENCES

T.M. Farabee and J.J. Casarella, “Spectral Features of Wall Pressure Fluctuations Beneath Turbulent Boundary Layers”, Physics of Fluids, **3**, 2410 (1991).

S. Gravante, A. Naguib, C. Wark and H. Nagib, “Characterization of the Pressure Fluctuations Under a Canonical Turbulent Boundary Layer,” AIAA Journal, **36** (10), 1808 (1998).

A. Honkan and J. Andreopoulos, “The Wall as a Source or Sink of Vorticity in Two Dimensional Turbulent Boundary Layer Flows,” in Near-Wall Turbulent Flows, RM.C. So, C.G. Speziale and B.E. Launder (Editors), Elsevier Science Publishers B.V. (1993).

L. Löfdahl, E. Kälvesten and G. Stemme, “Small Silicon Pressure Transducers for the Space-Time Correlation Measurements in a Flat Plate Boundary Layer,” FED-Vol. 197, Application of Microfabrication to Fluid Mechanics, ASME (1994).

A. Naguib, E. Soupos, H. Nagib, C.C. Huang and K. Najafi, “A Piezoresistive MEMS Sensor for Acoustic Noise Measurments,” 5th AIAA/CEAS Aeroacoustics Conference, AIAA Paper number 99-1992, Bellevue, Washington, May 10 – 12 (1999).

M. Sheplak, K.S. Breuer and M.A. Schmidt, “A Wafer-bonded, Silicon-nitride Membrane Microphone with Dielectrically-Isolated, Single-Crystal Silicon Piezoresistors,” Proceedings of the Solid-State Sensor and Actuator Workshop, Hilton Head, SC, June (1998).

S. Snarski and R.M. Lueptow, “Wall Pressure and Coherent Structures in a Turbulent Boundary layer on a Cylinder in an Axial Flow,” Journal of Fluid Mechanics, **286**, 137 (1995).